Electronic Supplementary Material (ESI) for Dalton Transactions.

Ru(II)/diclofenac-based complexes: DNA, BSA interaction and their anticancer evaluation against lung and breast tumor cells

Katia M. Oliveira[a,†,*], João Honorato[b,†], Guilherme R. Gonçalves[a], Marcia R. Cominetti[c], Alzir A. Batista[b], Rodrigo S. Correa[a,*]

[a]Departamento de Química, ICEB, Universidade Federal de Ouro Preto (UFOP), CEP 35400-000, Ouro Preto-MG, Brazil.

[b]Departamento de Química, Universidade Federal de São Carlos (UFSCar), Rodovia Washington Luiz, KM 235 CP 676, CEP 13561-901, São Carlos - SP, Brazil.

[c]Departamento de Gerontologia, Universidade Federal de São Carlos (UFSCar), Rodovia Washington Luiz, KM 235 CP 676, CEP 13561-901, São Carlos - SP, Brazil.

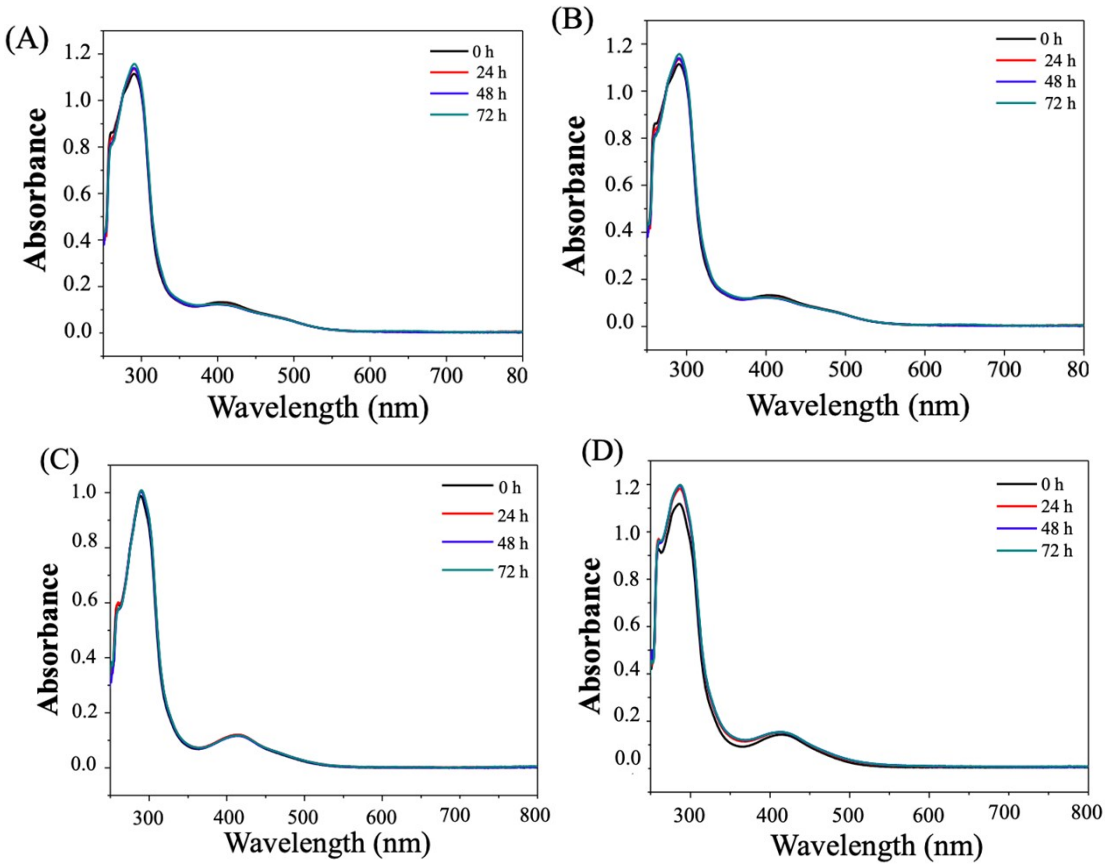

Figure S1. UV-Vis spectra of complexes (A) (**1**), (B) (**2**), (C) (**3**) and (D) (**4**), in DMSO at different times.

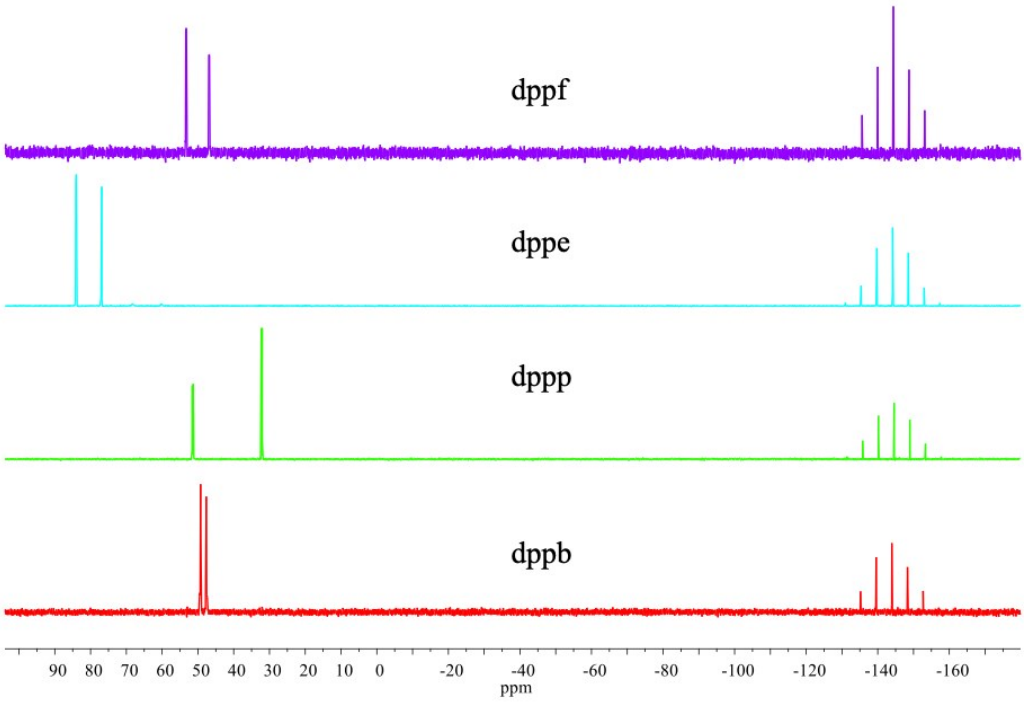

Figure S2. $^{31}P\{^{1}H\}$ NMR spectra of the complexes (**1**) dppb, (**2**) dppe, (**3**) dppp and (**4**) dppf, in CH_2Cl_2/D_2O.

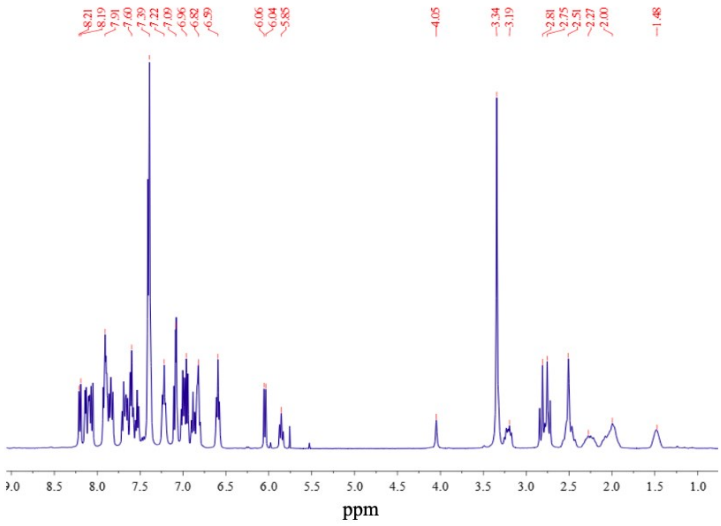

Figure S3. ^{1}H NMR spectrum of complex (**1**) in DMSO-d_6 at room temperature.

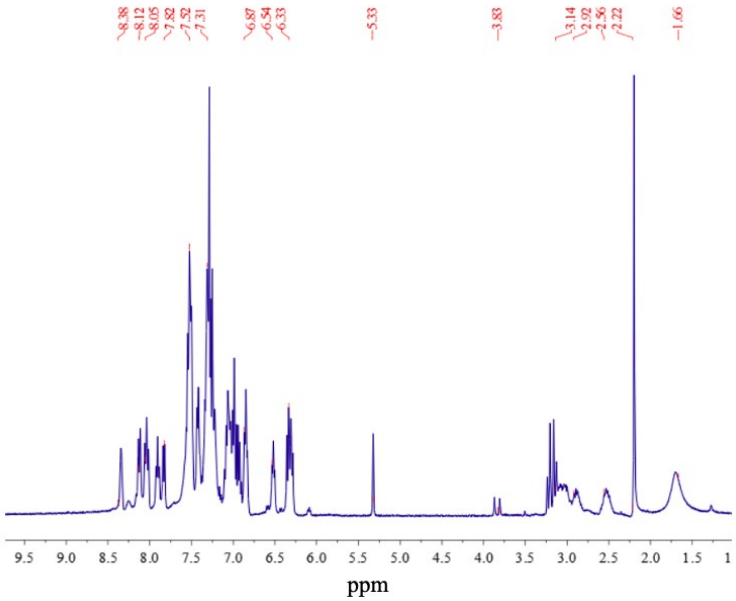

Figure S4. ^{1}H NMR spectrum of complex (**2**) in DMSO-d_6 at room temperature.

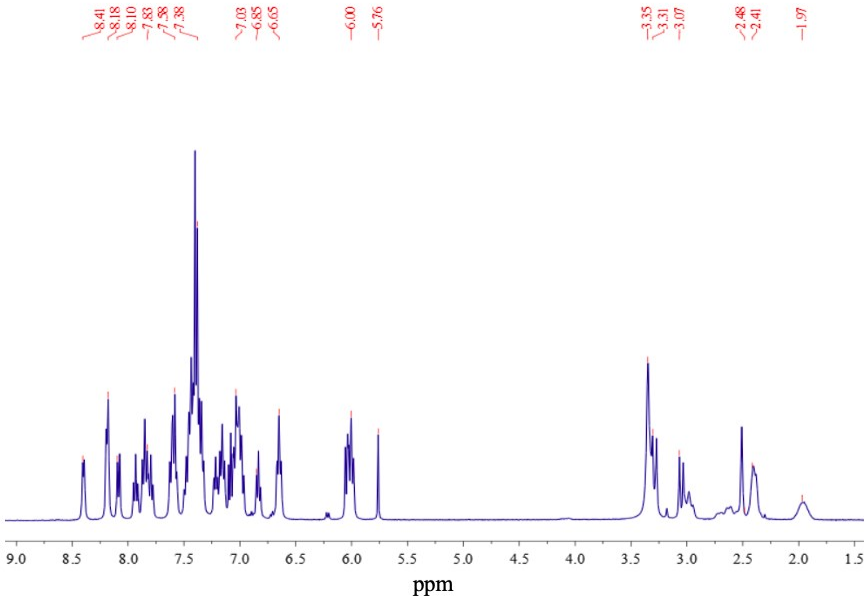

Figure S5. ^{1}H NMR spectrum of complex (**3**) in DMSO-d_6 at room temperature.

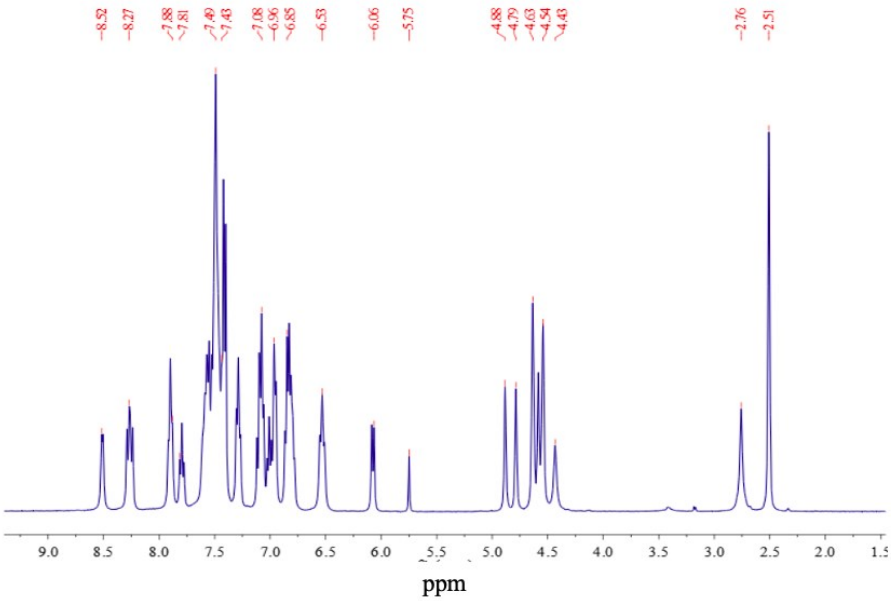

Figure S6. ^{1}H NMR spectrum of complex (**4**) in DMSO-d_6 at room temperature.

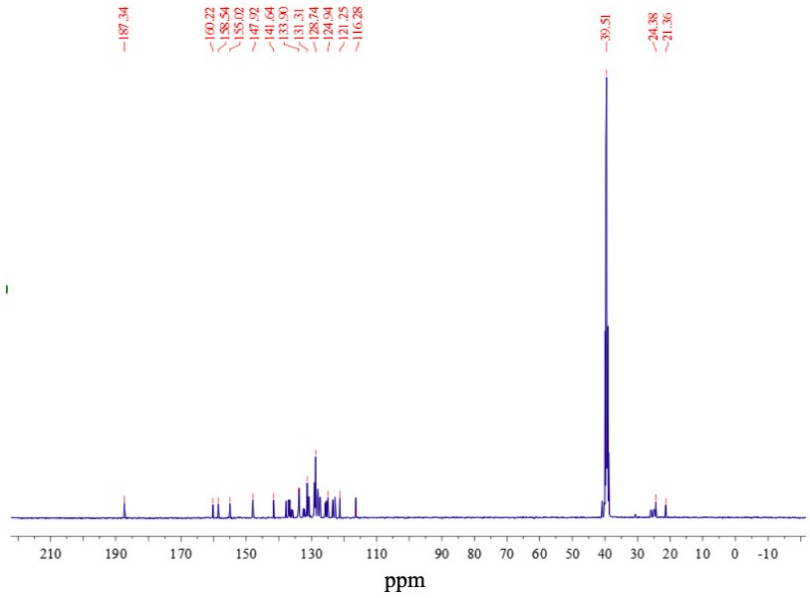

Figure S7. $^{13}C\{^{1}H\}$ NMR spectrum of complex (**1**) in DMSO-d_6 at room temperature.

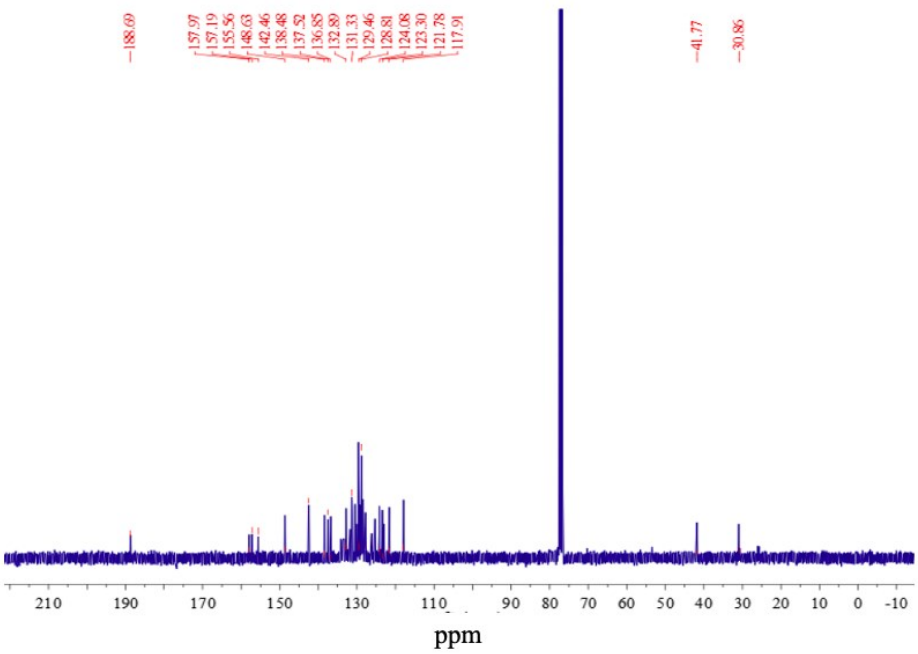

Figure S8. $^{13}C\{^{1}H\}$ NMR spectrum of complex (**2**) in DMSO-d_6 at room temperature.

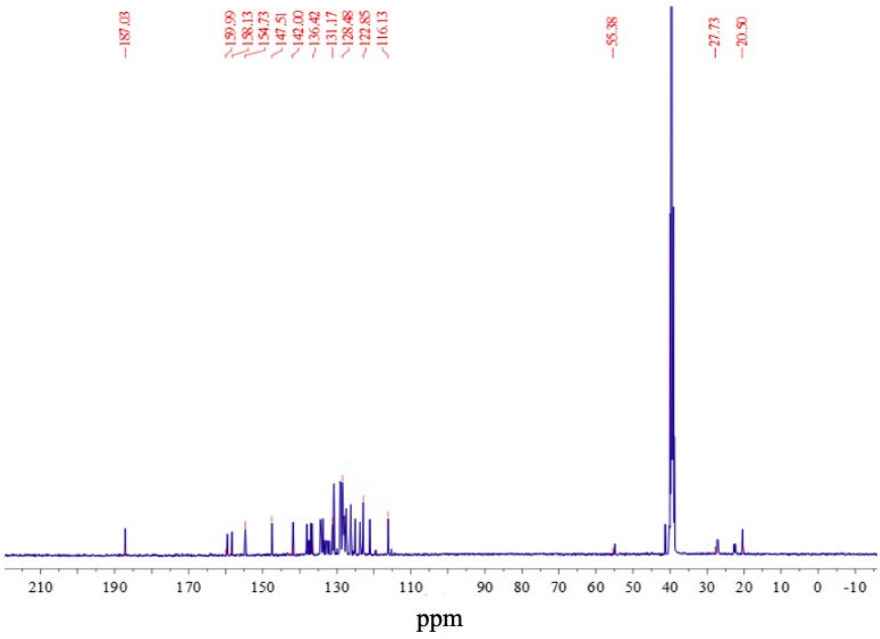

Figure S9. $^{13}C\{^{1}H\}$ NMR spectrum of complex (**3**) in DMSO-d_6 at room temperature.

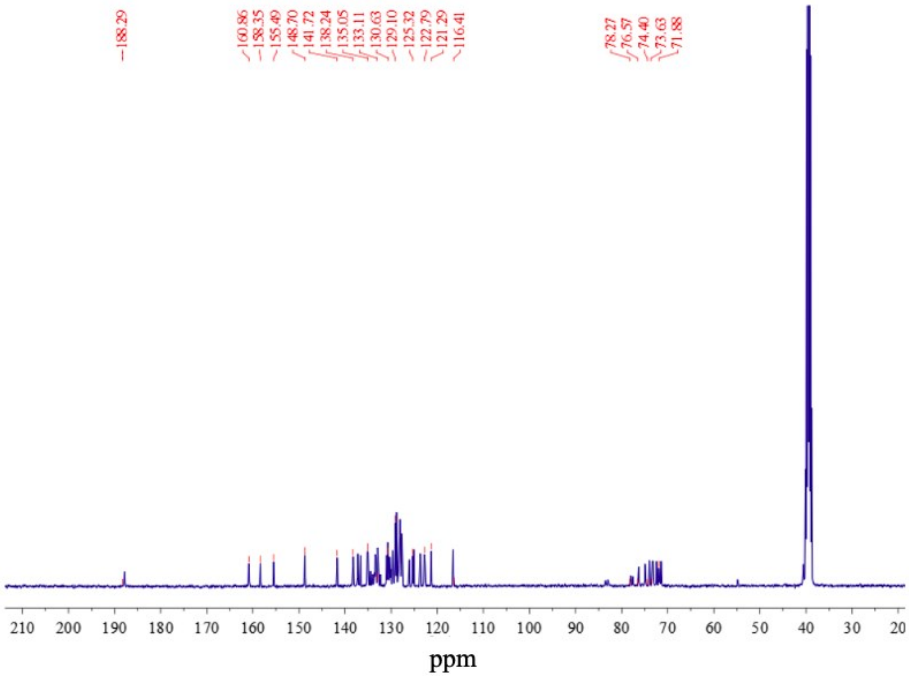

Figure S10. $^{13}C\{^{1}H\}$ NMR spectrum of complex (**4**) in DMSO-d_6 at room temperature.

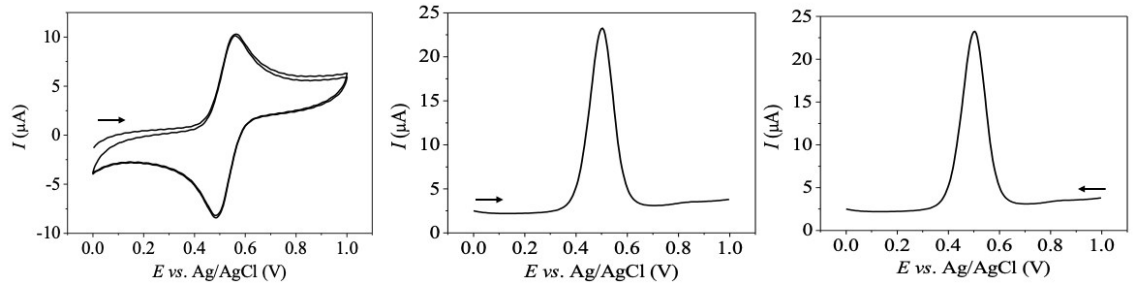

Figure S11. (**A**) Cyclic voltammogram and (**B**, **C**) differential pulse voltammogram of ferrocene (1×10^{-4} M). Electrolyte: 0.10 M $BuNClO_4$ in CH_2Cl_2; Electrodes: Pt disc as working and auxiliary and Ag/AgCl, as a reference; Scan rate: 50 mV s^{-1}.

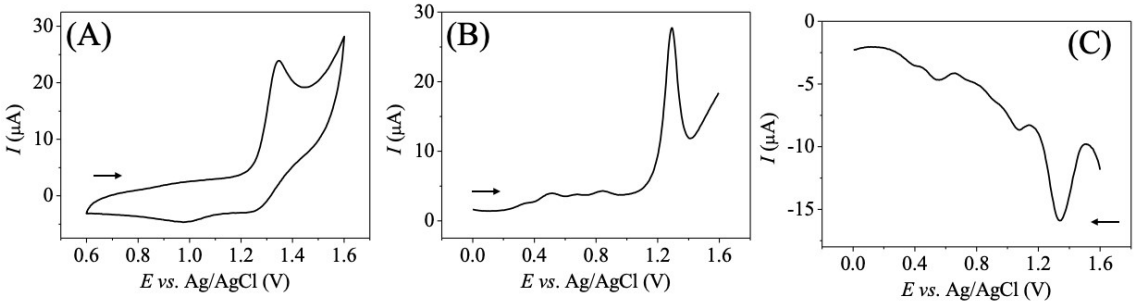

Figure S12. (**A**) Cyclic voltammogram and (**B**, **C**) differential pulse voltammogram of complex (**2**). Electrolyte: 0.10 M $BuNClO_4$ in CH_2Cl_2; Electrodes: Pt disc as working and auxiliary and Ag/AgCl, as a reference; Scan rate: 50 mV s^{-1}.

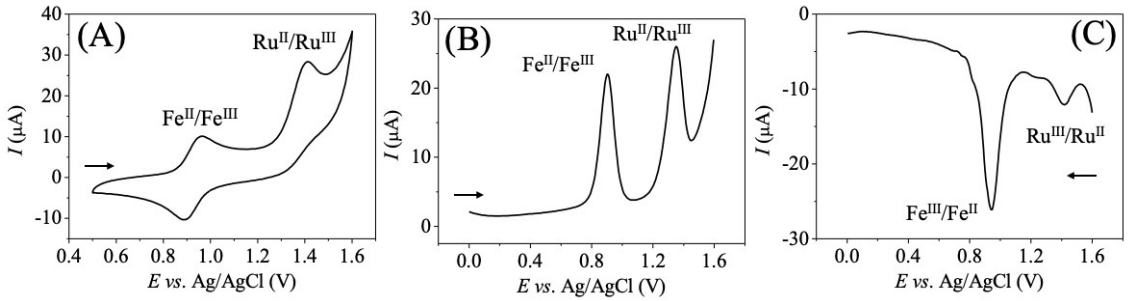

Figure S13. (**A**) Cyclic voltammogram and (**B**, **C**) differential pulse voltammogram of complex (**3**). Electrolyte: 0.10 M $BuNClO_4$ in CH_2Cl_2; Electrodes: Pt disc as working and auxiliary and Ag/AgCl, as a reference; Scan rate: 50 mV s^{-1}.

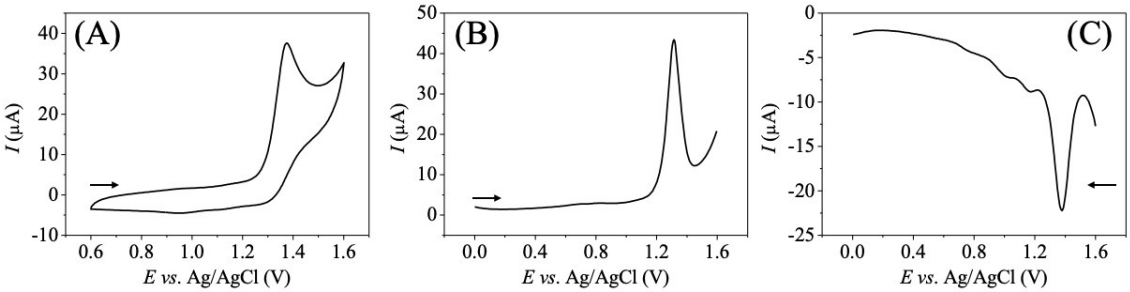

Figure S14. (**A**) Cyclic voltammogram and (**B**, **C**) differential pulse voltammogram of complex (**4**). Electrolyte: 0.10 M $BuNClO_4$ in CH_2Cl_2; Electrodes: Pt disc as working and auxiliary and Ag/AgCl, as a reference; Scan rate: 50 mV s^{-1}.

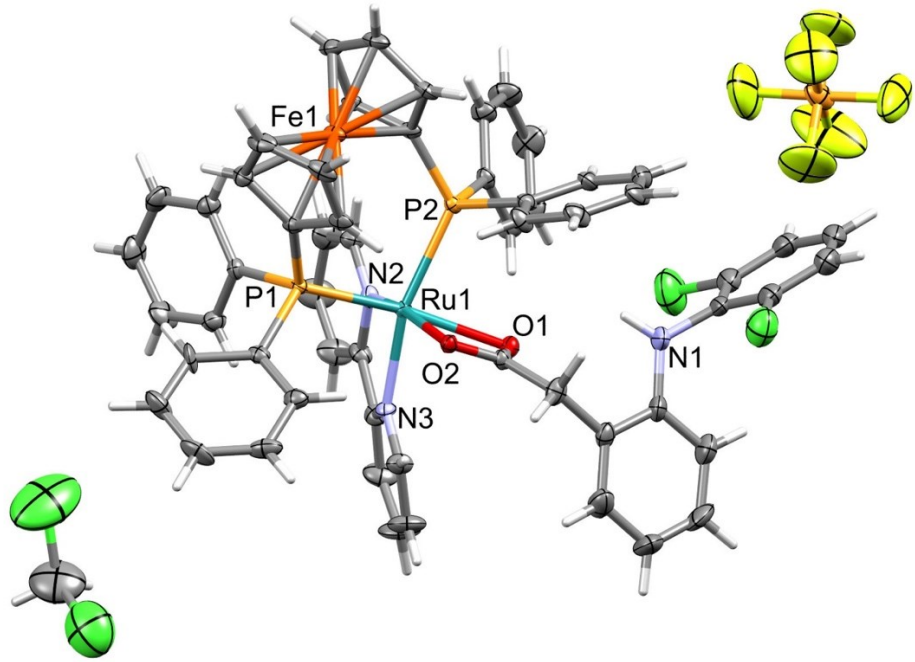

Figure S15. Crystal structure of complex (**4**).

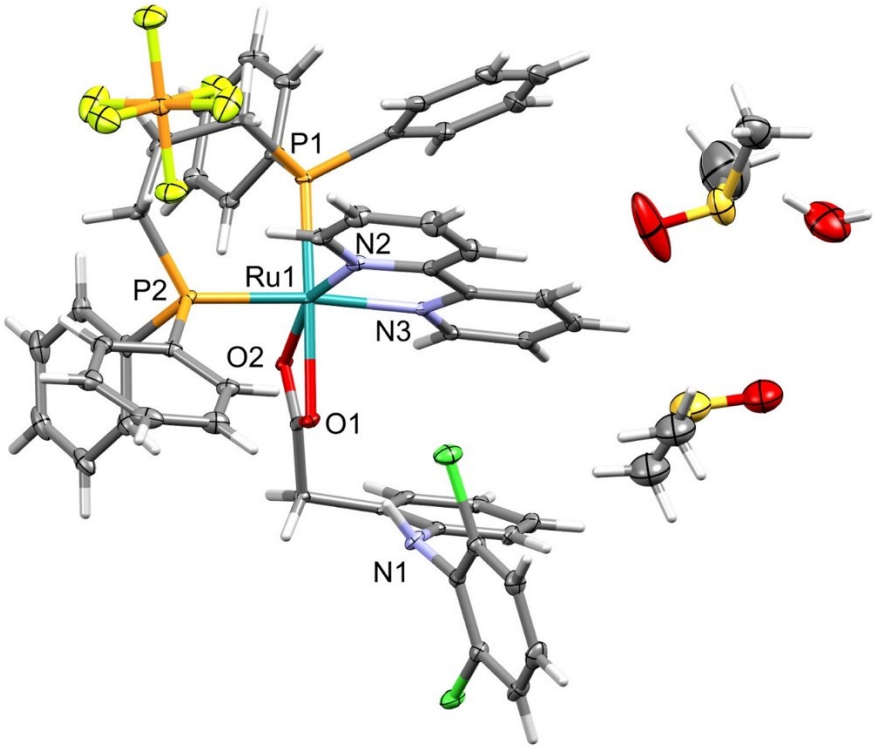

Figure S16. Crystal structure of complex (**3a**).

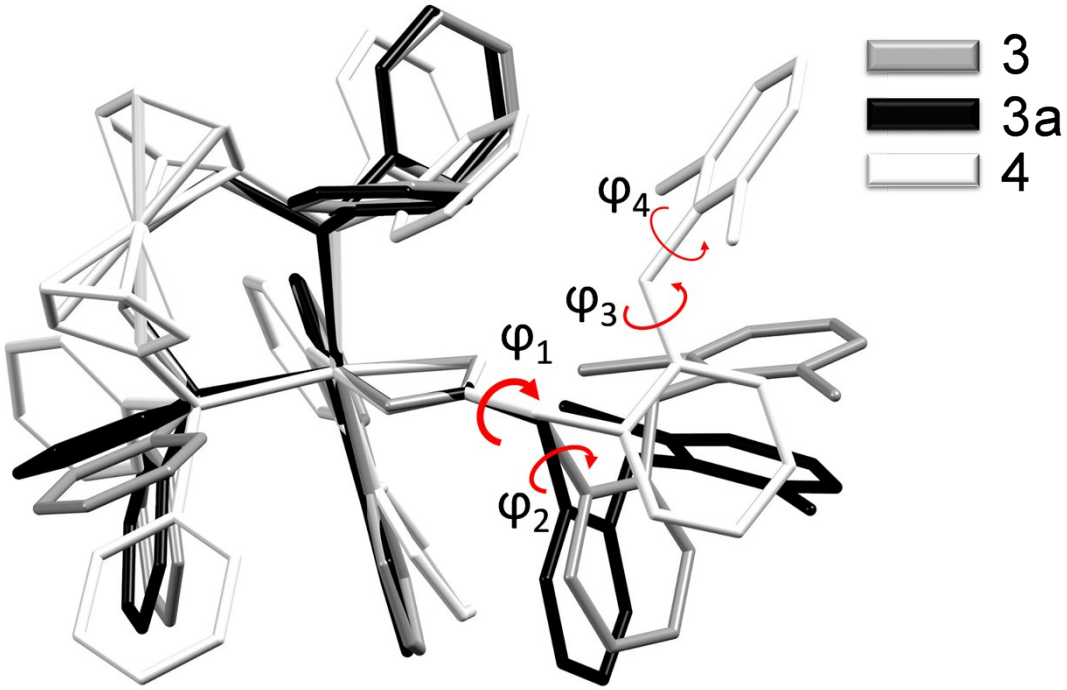

Figure S17. The overlap of the structures of complexes (**3**), (**3a**) and (**4**).

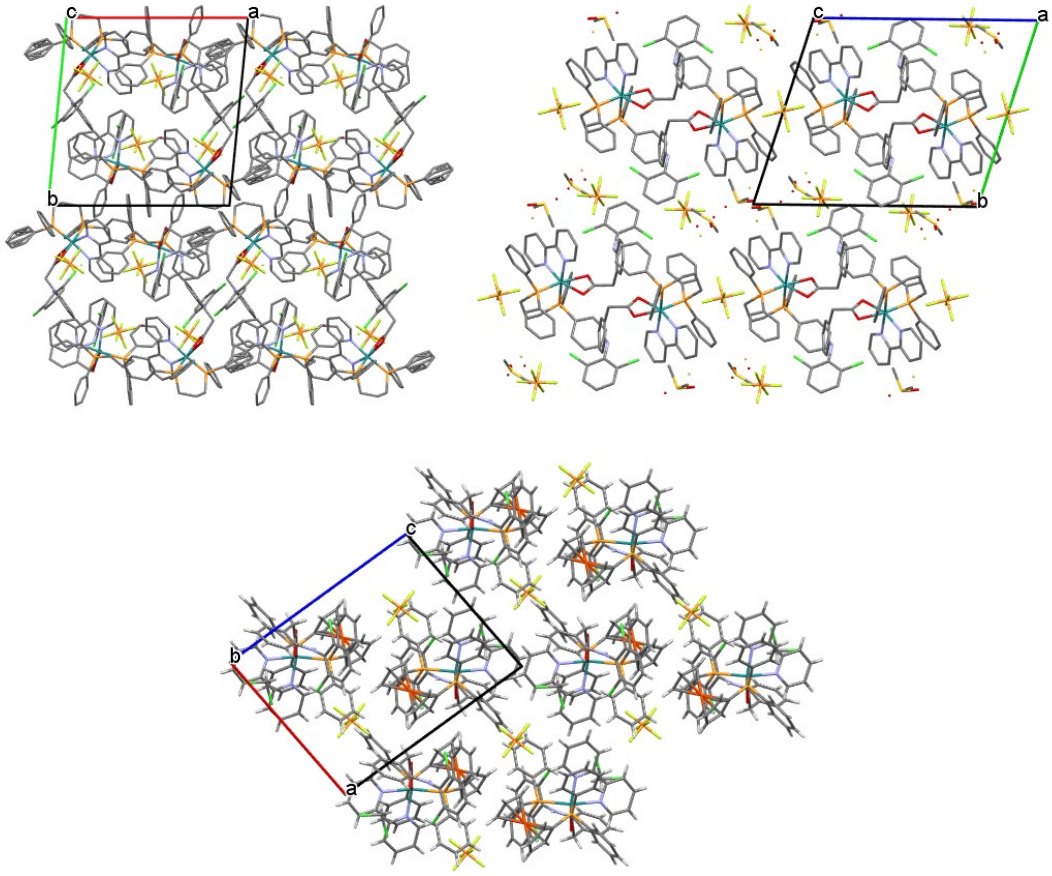

Figure S18. Crystal packing of complexes (**3**), (**3a**) and (**4**).

Table S1. Infrared assignment for complex (**1**) – (**4**).

Assignments	Complexes			
	1 /cm^{-1}	**2** /cm^{-1}	**3** /cm^{-1}	**4** /cm^{-1}
νNH	3256 sh;	3381 sh	3256 sh	3333 sh
νCH	3061, 2925 w	3054 w	3061w	3047 w
$\nu_{as}CH_2$	3074w	2835w	3074w	3074 w
$\nu_{s}CH_2$	2857 sh	2916 sh	2922 sh	2853 sh
$\nu C{=}C_{(anel)}$	1590 w	1598 s	1574 m	1565 m
$\nu C{=}C_{(anel)} + \nu C{=}C_{(fosf)}$	1481; 1443	1488; 1452 m	1486; 1464	1484; 1465 m
νC=C	1312 w	1308 w	1309 w	1305 w
νC-N	1234 m	1267 m	1274 m	1281 m
	1186; 1160w	1177; 1155 w	1189; 1156 w	1167 w
ν_{ass}P-CH	1090 m	1105 m	1094 m	1092 m
νAnel	996 w	999 w	999 w	1000 w
νP-F	838 s	833 s	835 s	828 s
δ N-H	905 w	956 w	964 w	958 w
δ CH_2	873 sh	879 sh	879 sh	893 sh
νC-Cl	763 m;	746 m	745 m	746 m
δP-CH e δP-CH_2	695 w	697 w	694 w	691 w
δP-F	552 m	571 m	579 m	557 m
$\nu_{as}(COO^-)$	**1502**	**1520**	**1506**	**1523**
$\nu_{s}(COO^-)$	**1448**	**1434**	**1434**	**1432**
[$\Delta\nu = \nu_{as}(COO^-) - \nu_{s}(COO^-)$]	**54**	**86**	**72**	**91**

s=Strong, m = media, w = weak, sh = shoulder

Table S2. X-Ray crystallographic data collection and refinement parameters for complex (**3**), (**3a**) and (**4**)

Identification code	**Complex 3**	**Complex 3a**	**Complex 4**
Empirical formula	$[RuC_{51}H_{44}Cl_2N_3O_2P_2]PF_6.½H_2O$	$[RuC_{54}H_{44}Cl_2N_3O_2P_2]PF_6.H_2O.2DMSO$	$[RuFeC_{58}H_{46}Cl_2N_3O_2P_2]PF_6.CH_2Cl_2$
CCDC	2000312	2000313	2000314
Formula weight	1103.77	1284.04	1315.66
Temperature	100(2) K	100(2) K	296(2) K
Wavelength	0.71073 Å	0.71073 Å	0.71073 Å
Crystal system	Triclinic	Triclinic	Triclinic
Space group	P -1	P -1	P -1
Unit cell dimensions	a = 16.821(3) Å; α= 106.108(2)°.	a = 11.441(2) Å, α= 70.244(3)°.	a = 13.9632(16) Å; α= 70.695(4)°.
	b = 17.342(3) Å; β= 107.431(2)°.	b = 15.858(3) Å, β= 79.049(3)°.	b = 14.6228(18) Å; β= 77.328(4)°.
	c = 18.540(3) Å; γ = 90.415(3)°.	c = 17.549(3) Å, γ = 71.215(3)°.	c = 16.5042(18) Å; γ = 64.054(4)°.
Volume	4933.1(13) $Å^3$	2825.3(8) $Å^3$	2848.7(6) $Å^3$
Z	4	2	2
Density (calculated)	1.486 Mg/m^3	1.509 Mg/m^3	1.534 Mg/m^3
Absorption coefficient	0.589 mm^{-1}	0.601 mm^{-1}	0.796 mm^{-1}
F(000)	2246	1316	1330
Crystal size	0.240 x 0.209 x 0.094 mm^3	0.182 x 0.079 x 0.063 mm^3	0.220 x 0.120 x 0.060 mm^3
Theta range for data collection	1.204 to 26.00°	1.238 to 25.50°.	1.312 to 25.05°.
Index ranges	-20≤h≤20, -21≤k≤21, -22≤l≤22	-13≤h≤13, -19≤k≤17, -21≤l≤21	-16≤h≤17, -17≤k≤18, 0≤l≤19
Reflections collected	36957	56357	9595
Independent reflections	19383 [R(int) = 0.0121]	10491 [R(int) = 0.0235]	9595 [R(int) = 0.1538]
Completeness to theta	99.9 %	99.8 %	95.0 %
Refinement method	Full-matrix least-squares on F^2	Full-matrix least-squares on F^2	Full-matrix least-squares on F^2
Data / restraints / parameters	19383 / 0 / 1283	10491 / 2 / 734	9595 / 0 / 713

Goodness-of-fit on F^2	1.039	1.036	1.075
Final R indices [I>2sigma(I)]	R1 = 0.0277, wR2 = 0.0711	R1 = 0.0617, wR2 = 0.1693	R1 = 0.1044, wR2 = 0.2578
R indices (all data)	R1 = 0.0311, wR2 = 0.0733	R1 = 0.0661, wR2 = 0.1748	R1 = 0.1122, wR2 = 0.2626
Largest diff. peak and hole	1.061 and -0.676 e.$Å^{-3}$	3.069 and -2.647 e.$Å^{-3}$	8.397 and -0.874 e.$Å^{-3}$

Table S3. Torsion angles of complexes (**3**), (**3a**) and (**4**)

Torsion angles (ϕ)/°	**3**	**3a**	**4**	**Ru-arene dicl [ref]**	**Potassium Diclofenac**	**Diclofenic acid, $P2_1/c$**	**Diclofenic acid, C2/c**
O1-C1-C2-C3	-66.49	-85.12	-26.27	-38.30	-57.70	-94.25	-109.81
C1-C2-C3-C4	81.66	74.00	78.34	74.40	78.15	79.19	81.51
C3-C4-N1-C9	175.29	163.00	159.52	166.33	164.18	162.81	165.52
C4-N1-C9-C10	-75.68	-60.12	-75.25	-65.53	-51.93	-63.41	-61.78